BIT
2002, Vol. 42, No. 1, pp. 194–205
0006-3835/02/4201-0194 $16.00

HOW MANY TIMESTEPS FOR A CYCLE? ANALYSIS OF THE WISDOM–HOLMAN ALGORITHM *

DIVAKAR VISWANATH

Departments of Mathematics, University of Michigan, Ann Arbor, MI 48109, USA.
email: divakar@umich.edu.

Abstract.

The Wisdom–Holman algorithm is an effective method for numerically solving nearly integrable systems. It takes into account the exact solution of the integrable part. If the nearly integrable system is the solar system, for example, the Wisdom–Holman algorithm uses the solution consisting of Keplerian orbits obtained when the interplanetary interactions are ignored. The effectiveness of the algorithm lies in its ability to take long timesteps. We use the Duffing oscillator and Kepler's problem with forcing to deduce how long those timesteps can be. For nearly Keplerian orbits, the timesteps must be at least six per orbital period even when the orbital eccentricity is zero. High eccentricity of the Keplerian orbits constrains the algorithm and forces it to take shorter timesteps. The analysis is applied to the solar system and other problems.

AMS subject classification: 65L05.

Key words: Ordinary differential equations, nearly integrable systems, Keplerian orbits, Hamiltonian.

1 Introduction.

The integration of the solar system by Sussman and Wisdom [11] is possibly the best known application of the Wisdom–Holman algorithm. The Hamiltonian governing the solar system can be written as $H_1 + \epsilon H_2$, where H_1 is mainly the interaction between the Sun and the planets, ϵ is a small parameter about a thousandth, and H_2 is mainly the interactions between the planets. Besides H_1 and H_2 are integrable by themselves. The way to write the Hamiltonian in such a form, though not difficult, is not entirely obvious and involves a passage to Jacobi coordinates.

The Wisdom–Holman algorithm [13] exploits this form of the Hamiltonian. A single timestep of size h is a half step of size $h/2$ under H_1 followed by a full step of size h under the perturbation ϵH_2 followed by another half step of size $h/2$ under H_2. This simple splitting algorithm is highly effective. Wisdom and Holman discovered this algorithm, and what is more, demonstrated its effectiveness by applying it to versions of the restricted three body problem and to integration of the outer solar system (Sun and planets from Jupiter to Pluto). The roots of this algorithm go back to a highly original paper by Wisdom [12].

*Received May 2000. Revised June 2001. Communicated by Olavi Nevanlinna.

The algorithm itself is of second order. However it can outperform conventional higher order methods with ease. McLachlan [4] points out that the order of local discretization error is not just Ch^3, as it is for any second order algorithm, but $\frac{1}{24}\epsilon h^3$. The presence of ϵ makes the algorithm very accurate. The accuracy of the algorithm can be further improved by applying symplectic correctors [15].

However, the order of accuracy alone cannot be a complete explanation of the success of this algorithm. The interest is in long term integrations. The Sussman–Wisdom integration [11] of the solar system is for 100 million years. There is an integration due to Laskar [7] for 15 billion years forwards and 10 billion years backwards. Laskar's method of integration requires initially an enormous symbolic computation specific to the solar system, tracks only the long period variation of orbital elements, but can take timesteps as long as 500 years! Using this method, Laskar discovered chaos in the inner solar system. Generally, the longer the integration the better and the integrations are typically run with nearly the longest timestep that is reliable. Sussman and Wisdom used a timestep of 7.2 days which is about 1/12th of the period of Mercury's orbit. Thus numerical stability is as much an issue as accuracy. Wisdom and Holman [13] state that "the map does not work well if fewer than five steps are taken per Jupiter orbit period", the problem being the integration of the outer solar system, and then again [14] that "the mapping method performed well provided that 10 or more mapping steps were taken for each mapping period". The purpose of this paper is to explain the numbers five and ten, and to uncover the dependence of how long the timesteps can be upon the eccentricity of the orbits.

The analysis in Sections 2 and 3 is based on the following very simple observation. There is an obvious and usually ineffective rule to perform the quadrature $\int_0^T \cos(\alpha t + \beta)dt$. The rule is to sample the function $\cos(\alpha t + \beta)$ at intervals of h, sum all the samples in $[0, T]$, and multiply by h. What length of the sampling interval ensures that the quadrature is roughly correct for increasing T? Though the question is imprecise, it is clear, for example, that if the sampling interval is exactly equal to the period $\frac{2*\pi}{\alpha}$, the quadrature will be meaningless—the sum will accumulate linearly instead of oscillating with T. If the sampling interval is one half of the period, it is possible that every sample is zero. However, if the sampling interval is a third of the period, the minimum sample over a length of time equal to the period is $-\frac{1}{2}$ or less, and the maximum is $\frac{1}{2}$ or more. Therefore, we assume that the sample and sum quadrature rule resolves a frequency only if it takes three or more timesteps per period. Later sections make frequent reference to this assumption.

The central issue in the analysis is related to stepsize resonance discovered and explained by Wisdom and Holman [14]. However, there are significant differences between the analysis here and that of Wisdom and Holman: firstly, the analysis here uses the simple observation above and not estimation of resonance widths and Chirikov's resonance overlap criterion; secondly, Wisdom and Holman do not explain the number of timesteps per orbit (for example, the numbers five and ten mentioned in a preceding paragraph) necessary for their algorithm to be meaningful. The focus here is on numerical stability exclusively. Stuart [10] surveys nonlinear stability analyses of several numerical schemes. The schemes considered by

Stuart are dissipative and the instabilities are exponential. The Wisdom–Holman algorithm is, obviously, symplectic and its instabilities are linear. The numerical stability analysis here ignores the symplectic character of the algorithm entirely.

Throughout this paper, for brevity, algorithm always refers to the Wisdom–Holman algorithm. Every other method is called a method or a scheme. Section 2 considers the Wisdom–Holman algorithm applied to the Duffing oscillator. It clarifies the basic issues and gives an outline of the approach, and can be considered a part of the introduction. Section 3 considers the algorithm applied to Kepler's problem with forcing. It shows that higher eccentricity of orbits forces the algorithm to take shorter timesteps to be numerically stable. Section 4 briefly considers some methods introduced by McLachlan [4]. Section 5 concludes.

2 The Duffing oscillator.

The Duffing oscillator is given by the equation

$$\ddot{q} = -q - \epsilon q^3.$$

The parameter ϵ is small (0.001 in this section), and the Duffing oscillator is only weakly nonlinear. Its Hamiltonian is $H_1 + \epsilon H_2$, where $H_1 = p^2/2 + q^2/2$ and $H_2 = \epsilon q^4/4$. The Wisdom–Holman algorithm takes a half step under H_1, a full step under ϵH_2, and then a half step under H_1. For purposes of analysis, here and in the rest of the paper, the trailing half step of the current step is fused with the leading half step of the next step, and a single step is taken to be a full step of ϵH_2 followed by a full step of H_1. This modified algorithm has local truncation error $O(\epsilon h^2)$ and is only first order. Obviously, if a timestep is numerically stable for the unmodified algorithm, it will be numerically stable for the modified algorithm, and vice versa. Though the analysis is framed for the modified algorithm, all the plots in this paper use the unmodified algorithm. The Duffing oscillator has a period of

$$2\pi\Big(1 - \frac{3}{8}\epsilon q_0^2\Big) + O(\epsilon^2)$$

for the initial condition $q = q_0$, $p = 0$ [5].

A step of size h under ϵH_2 is given by $p := p - h\epsilon q^3$. The coordinate q is unchanged. A step of size h under H_1 is given by

$$\begin{pmatrix} q \\ p \end{pmatrix} := \begin{pmatrix} \cos(h) & \sin(h) \\ -\sin(h) & \cos(h) \end{pmatrix} \begin{pmatrix} q \\ p \end{pmatrix},$$

a clockwise rotation of h in the q-p plane. But we prefer to interpret the algorithm after a time dependent change of variables. Pick variables r and T such that $q = r\cos(T - t)$ and $p = r\sin(T - t)$. The Duffing equation is

$$\begin{aligned} \dot{r} &= -\epsilon r^3 \sin(T-t)\cos^3(T-t) \\ &= -\epsilon r^3\Big(\frac{1}{4}\sin(2(T-t)) + \frac{1}{8}\sin(4(T-t))\Big), \\ \dot{T} &= -\epsilon r^2 \cos^4(T-t) \\ &= -\epsilon r^2\Big(\frac{3}{8} + \frac{1}{2}\cos(2(T-t)) + \frac{1}{8}\cos(4(T-t))\Big). \end{aligned} \tag{2.1}$$

In terms of r and T, a step of size h under H_1 at time t does not change r and T at all. The time is simply advanced from t to $t+h$. However, a step of size h under ϵH_2 changes r and T. Since the changes in p and q under that step are $\delta p = -h\epsilon q^3$ and $\delta q = 0$, the changes δr and δT are given by

$$\begin{aligned}\delta r &= \frac{\partial r}{\partial p}\delta p + O((\delta p)^2)\\ &= -h\epsilon r^3 \sin(T-t)\cos^3(T-t) + O(\epsilon^2 h^2),\\ \delta T &= \frac{\partial T}{\partial p}\delta p + O((\delta p)^2)\\ &= -h\epsilon r^2 \cos^4(T-t) + O(\epsilon^2 h^2).\end{aligned} \tag{2.2}$$

Up to a local error of $O(\epsilon^2 h^2)$, the modified algorithm is equivalent to the forward Euler method applied to (2.1). To infer this equivalence, compare (2.2) with one step of forward Euler for (2.1).

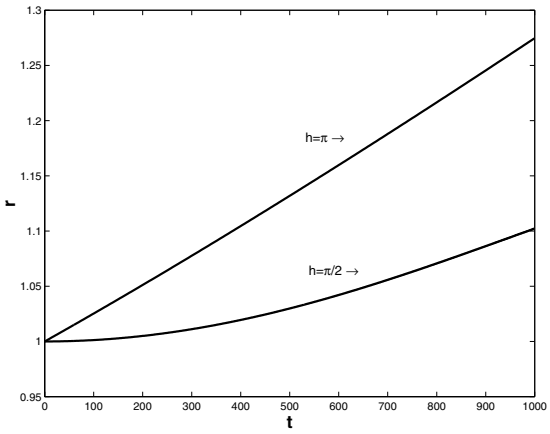

Figure 2.1: The Wisdom–Holman algorithm applied to the Duffing equation with stepsize h. The initial conditions were $p = q = 1/\sqrt{2}$, and ϵ was taken as 0.001. r does not oscillate with t as it should.

Because of this equivalence and the smallness of ϵ, the qualitative agreement with the exact solution will be the same for forward Euler applied to (2.1) with stepsize h and for the modified, or unmodified algorithm, with stepsize h. The limitations to the stepsize are easy to figure out for forward Euler applied to (2.1). Since r and T vary only by a small amount because ϵ is small, what is necessary is the proper resolution of the time dependent periodic terms. Those terms have periods π and $\pi/2$ in (2.1). Going back to the observation in the Introduction, the forward Euler method applied to (2.1) will cause r to increase or decrease steadily instead of oscillating when the stepsize is π or $\pi/2$. There are two approximations involved here. The first replaces the numerical stability analysis of the algorithm by the numerical stability analysis of forward Euler applied to (2.1). The second approximates forward Euler applied to (2.1) by forward Euler

applied to (2.1) but with the orbital elements, which vary slowly, fixed at their initial values, $r(T) = r(0)$ and $T(t) = T(0)$, while evaluating the right hand side. The last approximation is just a sample and sum quadrature.

See Figure 2.1. The stepsize of π samples both the terms $\sin(2(T-t))/4$ and $\sin(4(T-t))/8$ in (2.1) at a multiple of their periods. But the stepsize of $\pi/2$ samples only the latter at a multiple of its period. Thus the rate of increase of r with t for $h = \pi$ may be expected to be 3 times what it is for $h = \pi/2$, which it is roughly in Figure 2.1. The increase of r with t is not exactly linear in Figure 2.1 mainly because though r and T vary only slightly with t, they do vary with t, and the forward Euler method applied to (2.1) is really a nonlinear iteration. Another reason is that the Wisdom–Holman algorithm in the q-p plane is only approximately equivalent to forward Euler applied to (2.1).

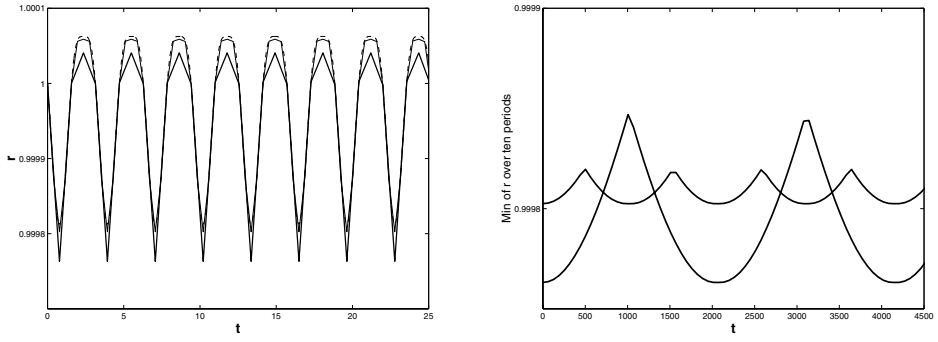

(a) (b)

Figure 2.2: The initial conditions and ϵ are the same as in Figure 2.1. In (a), the dashed line is the exact solution, the solid line uses $h = \pi/8$, and the thickest line uses $h = \pi/4$. The minimum of r taken over ten periods from t is a constant for the exact solution. However, in (b), there is a long period variation of this minimum with $h = \pi/8$ and $h = \pi/4$. The coarser stepsize causes a larger variation with a longer period.

Using the criterion stated in the introduction that three timesteps per period are needed to resolve a frequency, a safe stepsize for the Duffing equation is $h = \pi/6$ or shorter. Figure 2.2 (a) compares a stepsize of $\pi/8$ with a stepsize which is twice as long. But both those stepsizes give rise to long period variation as shown in Figure 2.2 (b). Taking $h = \pi/8.2$, for example, does away with this long period variation. The explanation for the long period variation of the minimum of r taken over ten periods from t with t shown in Figure 2.2 is simple. The equation for $\dot{T}$ in (2.1) has a term $-\epsilon r^2 3/8$ which is not periodic. This causes a secular (meaning slowly accumulating) change in T. We can take this into account by approximating the variation of r in the algorithm as given by forward Euler applied to $\dot{r} = -\epsilon r_0^3 \sin(T-t)\cos^3(4(T-t))$, where r_0 is the value of r at $t = 0$ and $T = T_0 - \frac{3}{8}\epsilon r_0^2 t$ and T_0 is the value of T at $t = 0$. This approximation incorporating the secular drift of T explains the long period variation for certain stepsizes shown in Figure 2.2. This long period variation is an example of an artifact whose cause is not stepsize resonance. Basically, stepsize resonance means that the stepsize is

equal or is a multiple of one of the periods in the disturbing function. For the Duffing oscillator, both $h = \pi$ and $h = \pi/2$ are resonant stepsizes, but $h = \pi/8$ is not a resonant stepsize.

Wisdom and Holman [14] use a delta function formulation of their algorithm to analyze stepsize resonances. The steps taken by the algorithm applied to $H_1 + \epsilon H_2$ matches the exact solution of the Hamiltonian

$$H_1 + \epsilon \delta_{2\pi}\Big(\frac{2\pi t}{h}\Big) H_2,$$

where $\delta_{2\pi} = \sum_{n=-\infty}^{\infty} \cos(nt)$ is a train of delta functions each of area 2π at intervals of 2π. The h in the modified Hamiltonian is the stepsize of the algorithm. The evolution under the modified Hamiltonian is thought of as flow under H_1 with periodic symplectic kicks from ϵH_2. For the Duffing oscillator, the symplectic kick changes p by $\Delta p = -h\epsilon q^3$ and leaves q unchanged. In order to carry out an analysis, they change variables so that H_2 can be written as a Poisson series. For the Duffing oscillator, this canonical change of variables is given by

$$J = (p^2 + q^2)/2 \quad \text{and} \quad \theta = \arctan(p/q).$$

The Hamiltonian becomes $J + \epsilon J^2 \cos^4(\theta)$ and the modified Hamiltonian is

$$J + \delta_{2\pi}\Big(\frac{2\pi t}{h}\Big) \epsilon J^2 \cos^4(\theta).$$

The symplectic kick that corresponds to this modified Hamiltonian is $\Delta\theta = h2\epsilon J \cos^4(\theta)$ and $\Delta J = h4\epsilon J^2 \cos^3(\theta)\sin(\theta)$.

These two symplectic kicks, one with q and p as the variables and the other with θ and J as the variables, are not the same. A simple calculation will show this. The standard theorem about transforming the Hamiltonian by simply substituting the new variables holds only assuming that the Hamiltonian is continuous and differentiable. It fails when the Hamiltonian has delta functions in it. This distinction between the two symplectic kicks is overlooked in [14] and [9]. Fortunately, this does not invalidate their analyses. The two symplectic kicks will match up to a local error of $O(\epsilon^2 h^2)$ and that order of match is good enough there as it is here. Thus both here and in the Wisdom–Holman paper, the iteration that is actually analyzed is slightly different from the algorithm.

3 Kepler's problem with forcing.

The unperturbed Duffing oscillator with $\epsilon = 0$ executes simple harmonic motion, and therefore, the dependence of the coordinates on time is composed of the basic frequency but not any of its multiples. However, when the eccentricity of Keplerian motion is not zero, the Fourier expansion of the coordinates and velocities in time has not only the basic frequency but all its integer multiples. The coefficients in the Fourier expansion fall off exponentially at a rate equal to the eccentricity. The presence of these higher frequencies can impose additional constraints on the Wisdom–Holman algorithm, especially when the eccentricity is close to 1. To

investigate the effect of these higher frequencies, we consider the model problem

$$\ddot{x} = -\frac{x}{(x^2+y^2)^{3/2}} + \delta\cos(\alpha t), \qquad \ddot{y} = -\frac{y}{(x^2+y^2)^{3/2}}, \tag{3.1}$$

which is Keplerian except for a periodic forcing term in the x direction. All the figures in this section use $\delta = 0.001$.

The algorithm is, in fact, always applied to problems which, unlike the model problem above, have no time dependence in the Hamiltonian. One step of the algorithm for this model problem at time t will first advance the velocity in the x direction as $\dot{x} := \dot{x} + h\delta\cos(\alpha t)$ followed by an exact Keplerian motion for duration h. The choice of the model problem greatly simplifies the expansion of the disturbing function, but still captures the constraints imposed by eccentricity upon the algorithm. Thus it can be used to gain understanding of the restrictions on the timestep of the algorithm.

Equation (3.1) uses Cartesian coordinates. Since the motion under (3.1) will be nearly Keplerian, it is useful to change variables to orbital elements. The four orbital elements used here a,e,ϵ, and w stand for semimajor axis, eccentricity, mean longitude at epoch, and longitude of the periapse, respectively. The conversion between Cartesian coordinates and orbital elements is discussed in several sources on celestial mechanics [1, 2, 3]. The intermediate variables mean anomaly M and the eccentric anomaly E are involved in passing back and forth between the two sets of variables. The mean anomaly at time t is given by $M = a^{-3/2}(t-T)$, where T is the time of passage through periapse. The eccentric anomaly is related to the mean anomaly by Kepler's equation $M = E - e\sin E$. To pass from the variables a, e, ϵ, w at time t to x, for example, the mean anomaly is computed as $M = \epsilon + a^{-3/2}t - w$, the eccentric anomaly is obtained from Kepler's equation, and finally x is computed from

$$x = a\cos w(\cos E - e) - a(1-e^2)^{1/2}\sin w\sin E.$$

If $\delta = 0$ in (3.1), the orbital elements would be constants of the motion. The variation of the orbital elements are caused by the periodic forcing term.

With minor changes to some details in Chapter 7 of Boccaletti and Puccaco [1], (3.1) can be written in terms of the orbital elements.

$$\begin{aligned}
\frac{da}{dt} &= 2a^{1/2}R_\epsilon,\\
\frac{de}{dt} &= -\frac{(1-e^2)^{1/2}}{a^{1/2}e}(1-(1-e^2)^{1/2})R_\epsilon - \frac{(1-e^2)^{1/2}}{a^{1/2}e}R_w,\\
\frac{d\epsilon}{dt} &= -2a^{1/2}R_a + \frac{(1-e^2)^{1/2}}{a^{1/2}e}(1-(1-e^2)^{1/2})R_e,\\
\frac{dw}{dt} &= \frac{(1-e^2)^{1/2}}{a^{1/2}e}R_e,
\end{aligned} \tag{3.2}$$

where $R_\theta = \delta\cos(\alpha t)\frac{\partial x}{\partial\theta}$ for θ equal to any one of a, e, ϵ, w. The Rs would be far more complicated if the perturbation in (3.1) were not so simple. Expanding x

as a Fourier series in the mean anomaly, plugging that Fourier series into (3.2), and retaining only the terms of the least degree in the eccentricity in the Fourier coefficients gives

$$\begin{aligned}\frac{da}{dt} = -4a^{3/2}\Big(&\frac{1}{2}\sin(M+w) + \frac{e}{2}\sin(2M+w) + \frac{9e^2}{16}\sin(3M+w)\\ &+ \frac{2e^3}{3}\sin(4M+w) + \frac{625e^4}{728}\sin(5M+w) + \frac{81e^5}{80}\sin(6M+w)\\ &+ \cdots\Big)\delta\cos(\alpha t)\end{aligned} \tag{3.3}$$

and

$$\begin{aligned}\frac{de}{dt} = 2a^{1/2}\Big(&\frac{3}{4}\sin w + \frac{e}{8}\sin(M-w) + \frac{1}{4}\sin(2M+w) + \frac{3e}{8}\sin(3M+w)\\ &+ \frac{e^2}{2}\sin(4M+w) + \frac{125e^3}{192}\sin(5M+w) + \frac{27e^4}{32}\sin(6M+w)\\ &+ \cdots\Big)\delta\cos(\alpha t).\end{aligned} \tag{3.4}$$

The Fourier series needed for the calculation above are given in Appendix D of [3] and, without any typos, in [2]. Equations (3.3) and (3.4) will be used to infer limitations on stepsizes, especially the limitations caused by high eccentricity. Since the orbital elements vary slowly, the mean anomaly is going to increase nearly at a rate given by $a^{-3/2}$, the orbital frequency. In all the figures in this section, α is $1/\sqrt{10}$ and δ is .001. Further, $a = 1$ at $t = 0$, which means that the forcing frequency is less than a third of the orbital frequency and that there is no resonance.

As was done for the Duffing oscillator, the nonlinear iteration of the algorithm applied to (3.1) can be approximated by forward Euler applied to (3.2) with the same stepsize. To understand the constraints on the stepsize of forward Euler, we make a further approximation, noting that the orbital elements vary only slowly. Forward Euler applied to (3.2), but with the orbital elements a, e, ϵ, w fixed at their starting values on the right hand side and the mean anomaly given by $M = \epsilon + a^{-3/2}t - w$, reduces to the sample and sum quadrature rule discussed in Section 1. From observing (3.3) and (3.4), it becomes clear that if the stepsize is not long enough the effect on the eccentricity should be more pronounced than the effect on the semimajor axis. The high frequency terms for de/dt have coefficients that are approximately $1/e$ times the coefficients in da/dt. Even when the eccentricity is very small, it follows from (3.4) that the timestep of the sample and sum quadrature rule must be small enough to resolve twice the orbital frequency. Thus even though the eccentricity of Jupiter at 0.048 is quite close to zero, the algorithm should be expected to "not work well if fewer than five steps are taken per Jupiter orbit period" in an integration of the outer solar system. Since at least three steps per period are necessary to resolve a frequency, the stepsize must be at least a sixth of Jupiter's period.

When the eccentricity is not exactly zero, the right hand side of (3.4) has not just the orbital frequency, but all integer multiples of it. However, not every

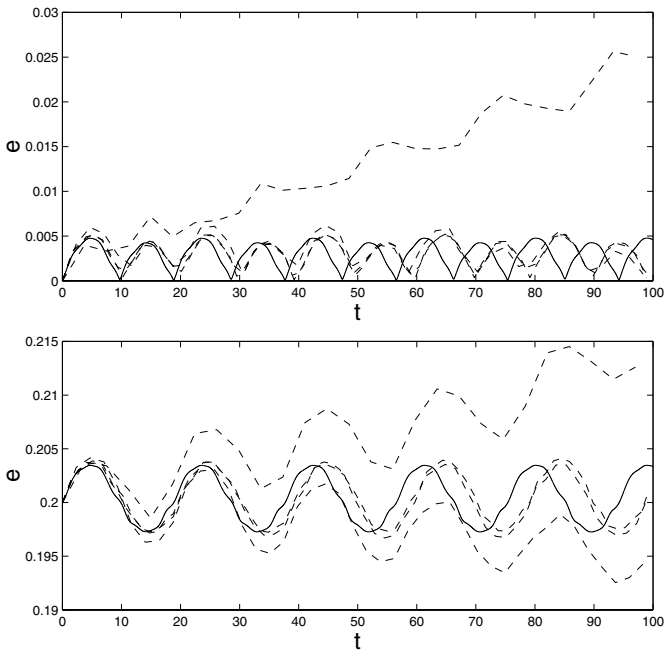

Figure 3.1: The initial conditions are given by $a = 1$, $\epsilon = \pi/4$, $w = -\pi/4$, and $e = 0$ above and $e = 0.2$ below. The thick lines give nearly the exact variation of eccentricity e with time. The dashed lines are approximations computed using the Wisdom–Holman algorithm with stepsizes of $2\pi/(2-\alpha)$, $2\pi/(3-\alpha)$, $2\pi/(4-\alpha)$, and $2\pi/(5-\alpha)$, where $\alpha = 1/\sqrt{10}$.

frequency needs to be resolved. The coefficients of the higher frequencies decrease exponentially at a rate give by e. Even if some of these frequencies are aliased to lower frequencies, this will not cause any harm if the coefficients are small enough. But how many frequencies should be resolved? The only thing that can be said with certainty is that higher the eccentricity the greater the need to resolve the higher frequencies; see Figure 3.1. When $e = 0$, resonant sampling with the stepsize $2\pi/(2-\alpha)$ of $\sin(2M + w)\cos(\alpha t)$ has a very pronounced effect, but the other stepsizes appear stable. When $e = 0.2$, resonant sampling with stepsize $2\pi/(3-\alpha)$ of $\sin(3M + w)\cos(\alpha t)$ causes a smaller but still pronounced effect. Thus that frequency too should probably be resolved when $e = 0.2$.

Figure 3.2 compares the approximations used here with the Wisdom–Holman algorithm. As may be expected, applying forward Euler to (3.2) with the orbital elements frozen at their starting values causes a clear instability that increases linearly with time. The instability of forward Euler approximates the instability of the algorithm quite well. But the beginning trend of the instability in all the three cases is linear, and the magnitude of the slope of this linear trend is roughly the same in all three cases. The variation of the orbital element ϵ is small when $t \ll 1/\delta$ naturally, but the terms in $\frac{d\epsilon}{dt}$ are not all periodic in t. Because of this ϵ does not

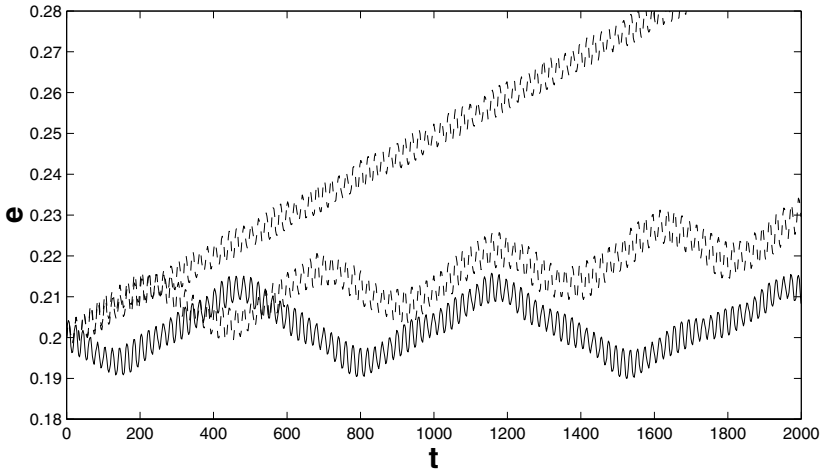

Figure 3.2: The thick line corresponds to the Wisdom–Holman algorithm with initial conditions $a = 1$, $e = 0.2$, $\epsilon = \pi/4$, and $w = -\pi/4$. The dashed lines correspond to forward Euler applied (3.2) and to forward Euler applied to (3.2) with the orbital elements frozen at their starting values. The latter is the most unstable of the three.

Table 3.1: Estimates and actual slopes for stepsizes $2\pi/(N-\alpha)$ with $N = 2, 3, 4, 5, 6$.

N	slope of linear instability	estimate of slope
2	$1.59e-4$	$6.70e-5$
3	$4.86e-5$	$3.20e-5$
4	$1.28e-5$	$1.17e-5$
5	$3.32e-6$	$3.88e-6$
6	$8.53e-7$	$1.22e-6$

just oscillate about its initial value like a and e in the exact solution, but drifts away gradually from its starting value. Our explanation of the instability is based on summing samples of $\sin(3M+w)\cos(\alpha t)$, where $M = \epsilon + a^{-3/2}t - w$, chosen at intervals of $2\pi/(3a^{-3/2}-\alpha)$. That explanation predicts a linearly increasing instability, but the prediction will hold only as long as the variation in ϵ is not too much. As ϵ drifts away, it changes the phase of M but the sampling continues at the same phase. This mechanism by which the mean anomaly M and the sampling points drift in and out of phase slowly stabilizes both the forward Euler applied to (3.2) and the algorithm, and prevents the linear trend of the instability from continuing indefinitely.

A least squares fit gives the slope of the linear instability in Figure 3.2 as $4.86e{-}5$. The coefficient of $\sin(2M+w)\cos(\alpha t)$ in (3.4) is $3\delta a^{1/2}e/4$. If the instability were caused by sampling this term alone with a stepsize of $h = 2\pi/(3-\alpha)$, its slope would be approximately $3\delta a^{1/2}e/(8h)$ or $3.2e{-}5$. Table 3.1 compares the estimates with the actual slopes for stepsizes $2\pi/(N-\alpha)$ with $N = 2, 3, 4, 5, 6$.

Rauch and Holman [9] have studied the Wisdom–Holman algorithm applied to the Stark problem. Taking $\alpha = 0$ in (3.1) gives an instance of the Stark problem. The eccentricity can increase to 1 and decrease and then increases again and so on. They find that the algorithm does not perform satisfactorily however small the stepsize. From the point view of this paper, more and more higher frequencies need to be resolved as the eccentricity approaches 1, as is evident from (3.4), and when the eccentricity is very close to 1 even very small stepsizes probably will not be numerically stable. A regularization of the Wisdom–Holman algorithm due to Mikkola [8] can handle the Stark problem.

4 McLachlan's method.

McLachlan [4] introduces several methods for integrating motion under Hamiltonians of the form $H_1 + \epsilon H_2$, where both H_1 and H_2 are integrable. A step of size h under one of these methods is a step of size $h/6$ under ϵH_2, followed by a step of $h/2$ under H_1, followed by a step of $2h/3$ under ϵH_2, followed by a step of $h/2$ under H_1, followed by a step of $h/6$ under ϵH_2. The local truncation error of this method, $O(\epsilon^2 h^3)$, is smaller than the local truncation error of the Wisdom–Holman algorithm by a factor of ϵ.

To understand the numerical stability of this method, the nonlinear iteration when the method is applied to the Duffing oscillator is approximated by another nonlinear iteration in terms of the variables r and T in (2.1). The approximating iteration will change r and T using a forward Euler step of $h/6$ applied to (2.1) at time t, advance time to $t + h/2$, change r and T using a forward Euler step of $2h/3$, advance time to $t + h$, and change r and T again using a forward Euler step of $h/6$. If the variation in r and T is ignored in evaluating the right hand side of (2.1) during the Euler steps, the iteration becomes an approximate quadrature. If such an iteration were used to perform quadrature of the function $\cos(t)$, it would appoximate $\sin(nh)$ as $-\frac{1}{6} + \cos(nh)/6 + \sum_{k=0}^{n-1} \frac{1}{3}\cos(kh) + \frac{2}{3}\cos(kh + h/2)$. When $h = 2\pi$, for example, there will be a linear instability. Its slope will be a third of the slope when the samples are taken at intervals of h and added. However, a step of h under this method costs twice as much as a step of size h under the Wisdom–Holman algorithm. So it does not seem to have a clear advantage or disadvantage as far as numerical stability is concerned.

5 Conclusion.

The 100 million year integration of the solar system by Sussman and Wisdom [11] used a stepsize of 7.2 days. This is about a 1/12th of Mercury's orbital period. Given that Mercury's eccentricity is close to 0.2, it is unlikely that a stepsize of a sixth of Mercury's orbital period, the maximum possible stepsize according to Section 3, would be numerically stable. The stepsize of 7.2 days resolves up to four times the orbital frequency. From (3.4), the coefficient of $\sin(5M + w)$, the term corresponding to the first unresolved frequency, is only 2% of the coefficient of $\sin(2M + w)$ for $e = 0.2$.

Wisdom, Holman, and Touma [15] have derived symplectic correctors to eliminate oscillatory errors whose period is equal to the stepsize. They say that improvement in accuracy from using symplectic correctors would be more dramatic if the stepsize in the solar system integration were half of 7.2 days. Since the errors introduced by frequencies left unresolved by coarse stepsizes increase linearly and oscillate with periods much longer than the stepsize as shown in Section 3, the symplectic correctors will not be able to eliminate these errors. It is quite possible that errors from under-resolved frequencies can explain the diminished effectiveness of symplectic correctors at coarse stepsizes. However, an analysis needs to be done to confirm this possibility.

The title to this paper asks how many timesteps for a cycle? Section 2 showed that the Wisdom–Holman algorithm applied to the Duffing oscillator must use at least 12 timesteps per cycle. Section 3 showed that if the orbit is nearly Keplerian, the algorithm must use at least 6 timesteps per orbital period.

REFERENCES

1. D. Boccaletti and G. Pucacco, *Theory of Orbits*, Vol. 2, Springer-Verlag, New York, 1998.
2. D. Brouwer and G. M. Clemence, *Methods of Celestial Mechanics*, Academic Press, New York, 1961.
3. J. M. A. Danby, *Fundamentals of Celestial Mechanics*, 2nd ed., Willman-Bell, Richmond, VA, 1988.
4. R. I. McLachlan, *Composition methods in the presence of small parameters*, BIT, 35 (1995), pp. 258–268.
5. A. H. Nayfeh, *Introduction to Perturbation Techniques*, Wiley, New York, 1993.
6. J. Laskar, *A numerical experiment on the chaotic behaviour of the solar system*, Nature, 338 (1989), pp. 237–238.
7. J. Laskar, *Large-scale chaos in the solar system*, Astron. Astrophys., 287 (1994), pp. L9–L12.
8. S. Mikkola, *Practical symplectic methods with time transformation for the few-body problem*, Celest. Mech. Dynamic Astron. 67 (1997), p. 145–165.
9. K. P. Rauch and M. Holman, *Dynamical chaos in the Wisdom–Holman integrator: Origins and solutions*, Astron. J., 117 (1999), pp. 1087–1102.
10. A. M. Stuart, *Nonlinear instability in dissipative finite difference schemes*, SIAM Review, 31 (1989), pp. 191–220.
11. G. J. Sussman and J. Wisdom, *Chaotic evolution of the solar system*, Science, 257 (1992), pp. 56–62.
12. J. Wisdom, *The origin of the Kirkwood gaps: A mapping for asteroidal motion near the 3/1 commensurability*, Astron. J., 87:3 (1982), pp. 577–593.
13. J. Wisdom and M. Holman, *Symplectic maps for the N-body problem*, Astron. J., 102:4 (1991), pp. 1528–1538.
14. J. Wisdom and M. Holman, *Symplectic maps for the N-body problem: Stability analysis*, Astron. J., pp. 104:5 (1992), pp. 2022–2029.
15. J. Wisdom, M. Holman, and J. Touma, *Symplectic correctors*, in Integration Algorithms and Classical Mechanics, Fields Institute Comm., Vol. 10, American Mathematical Society, Providence, RI, 1996, p. 217.